MEaSUREs (Making Earth System Data Records for Use in Research Environments)

Low Earth Orbit Land Surface Temperature Product (LEO-LST) User Guide and Algorithm Theoretical Basis Document

Glynn Hulley, Simon Hook, Kerry Cawse-Nicholson, Robert Freepartner

Jet Propulsion Laboratory, California Institute of Technology

Change History Log

Revision	Effective Date	Prepared by	Description of Changes
1.0	04/25/2022	Glynn Hulley	User Guide/ATBD first draft

Product Versions

Version	Effective Date	DOI	Description of Changes
1.0	08/15/2022	https://doi.org/10.5067/MEaSUREs/LSTE/LEOLSTCMG30.001	First version with data from 2002-08-01 to 2022-08-01
2.0	10/01/2023	https://doi.org/10.5067/MEaSUREs/LSTE/LEOLSTCMG30.002	Fixed issue with nighttime LST error estimates set to all zeros. Extended dataset until 2022-12-31

Contacts

Readers seeking additional information about this product may contact the following:

- Glynn Hulley
  MS 183-501
  Jet Propulsion Laboratory
  4800 Oak Grove Dr.
  Pasadena, CA 91109
  Email: glynn.hulley@jpl.nasa.gov
  Office: (818) 354-2979

Contents

List of figures

List of tables

1 Introduction

This is the user guide for the MEaSUREs (Making Earth System Data Records for Use in Research Environments) Land Surface Temperature (LST) product derived from the Low Earth Orbit (LEO) satellite data record from the MODIS and VIIRS instruments. The LEO-LST product will include global LST produced on climate modeling grids (CMG) on monthly timesteps from 2002-2029. This is version 1.0 of the ATBD and the goal is maintaining a 'living' version of this document with changes made when necessary.

Land Surface Temperature and Emissivity (LST&E) are critical variables used in a wide range of Earth science studies. They are necessary inputs for surface energy balance models used in drought monitoring, soil moisture estimation, and monitoring water consumptive use (Anderson et al. 2011a; Hain et al. 2011; Semmens et al. 2016). They are used for the retrieval of climate variables such as tropospheric water vapor and air temperature (Seemann et al. 2008; Susskind and Blaisdell 2008; Yao et al. 2011). They are also used to monitor climate warming trends (Hall et al. 2012; Schneider and Hook 2010), measure the urban heat island effect (Dousset and Gourmelon 2003; Luvall et al. 2015) and heat waves (Dousset et al. 2011; Luvall et al. 2015), detect land cover and land use change (French et al. 2008; Hulley et al. 2014a), and map surface composition (Hook et al. 2005; Vaughan et al. 2005).

NASA has identified LST&E data as an important Earth System Data Record (ESDR) (NASA 2005, 2011) along with other international organizations (e.g. Global Climate Observing System (GCOS), 2003; Climate Change Science Program (CCSP), 2006). LST was recently designated as an Essential Climate Variable (ECV) by GCOS and several international initiatives have been established to utilize LST&E data including the EarthTemp network (http://www.earthtemp.net/), GlobTemperature (http://www.globtemperature.info/) and the International Land Surface Temperature and Emissivity Working Group (ILSTE-WG, http://ilste-wg.org/).

LST&E products from MODIS (MxD21) and VIIRS (VNP21) are currently produced operationally by NASA on daily timescales using thermal infrared (TIR) data in the 8-13 µm range from the MODIS instruments on the NASA-EOS platforms (Aqua, Terra) at 1-km spatial resolution at nadir (Hulley et al. 2017; Malakar and Hulley 2016), and from moderate resolution TIR bands (M-bands) from the VIIRS instrument on the Suomi-NPP (SNPP) platform at 750-m spatial resolution (Hulley et al. 2017; Islam et al. 2017). These products are generated using a consistent Temperature Emissivity Separation (TES) algorithm to physically retrieve both LST and spectral emissivity consistently for both sensors with high accuracy and well defined uncertainties (Islam et al. 2017). A study led by PI Hulley demonstrated continuity between the MYD21 (MODIS Aqua) and VNP21 LST products at the $<\pm0.5$ K level in LST RMSE, with differences that are invariant to environmental conditions and land cover type (Hulley et al. 2017). Continuity between the MODIS and VIIRS LST&E products will ensure a consistent and well characterized long term LST&E data record for better monitoring and understanding trends in Earth system behavior.

The MEaSUREs LEO-LST product will be generated by regridding the monthly Climate Modeling Grid (CMG) products from MODIS-Aqua (MYD21 from 2002) and VIIRS on SNPP (VNP21 from 2011) and NOAA-20 (VJ121 from 2018) and making them available on 0.25, 0.5, and 1 degree optimized climate grids with well characterized per-pixel uncertainties. During overlap years, i.e. MYD21 and VNP21 from 2011 onward, and for VNP21 and VJ121 from 2023

onward (at the end of MODIS-Aqua) we will merge the two products using a 'combination of states of information' approach to provide a long-term well calibrated and consistent LST record at 1-km resolution on monthly timesteps.
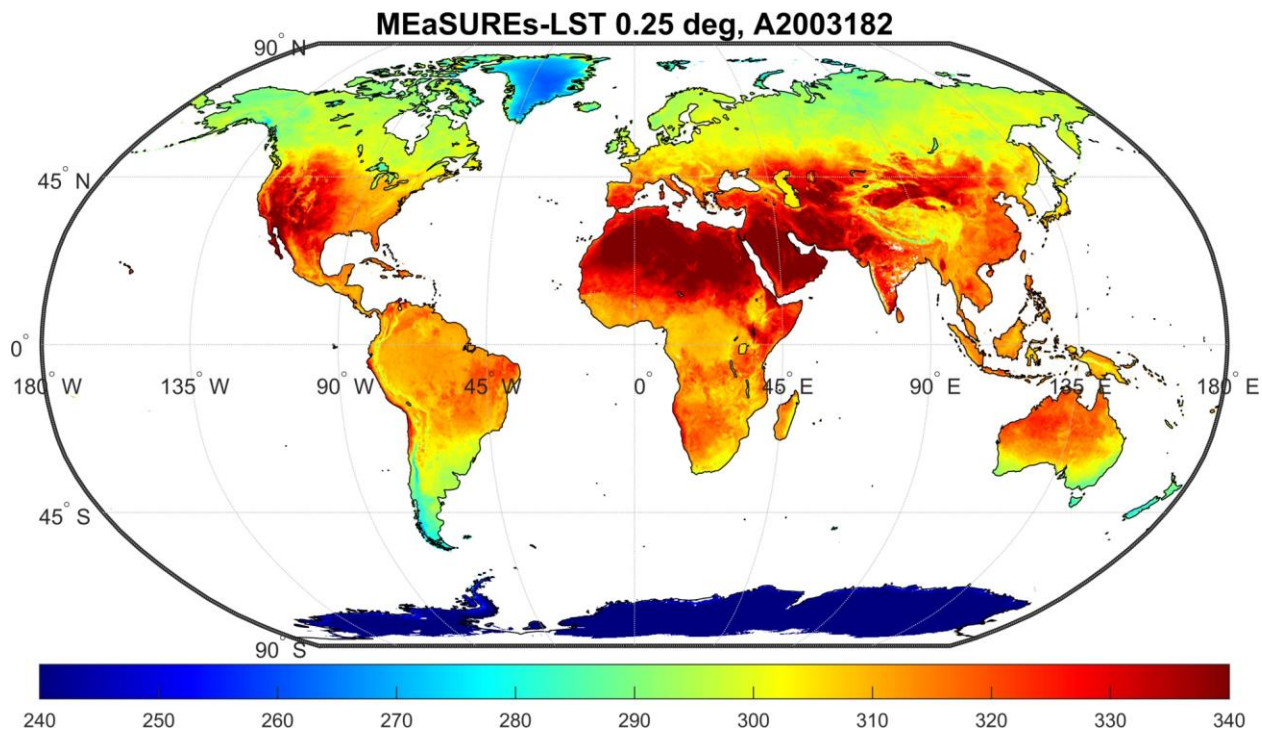
Figure 1. An example LEO-LST gridded daytime image at 0.25 degree resolution for July 2003.

The long-term MODIS-VIIRS LST record will be of use to the global climate modeling community, for example in Observations for Model Intercomparisons Project (obs4mips). Obs4mips is an activity to make observational products such as LST more accessible for climate model intercomparisons and evaluation. It provides data specifications that are closely aligned with the Coupled Model Intercomparison Project (CMIP) making it possible to make data available via the same searchable distributed system used to serve and disseminate the rapidly expanding set of simulations made available for community research.

1.1 File format

The LEO-LST products are distributed in HDF5 format and can be read in by HDF5 software. Information on Hierarchical Data Format 5 (HDF5) may be found at https://www.hdfgroup.org/HDF5/. The HDF format was developed by NCSA and has been widely used in the scientific domain. HDF5 can store two primary types of objects: datasets and groups. A dataset is essentially a multidimensional array of data elements, and a group is a structure for organizing objects in an HDF5 file. HDF5 was designed to address some of the limitations of the HDF4. Using these two basic objects, one can create and store almost any kind of scientific data structure, such as images, arrays of vectors, and structured and unstructured

grids. They can be mixed and matched in HDF5 files according to user needs. HDF5 does not limit the size of files or the size or number of objects in a file. The scientific data results are delivered as SDSs with local attributes including summary statistics and other information about the data.

The LEO-LST data product files contain one set of Attributes (metadata) describing information relevant to production, archiving, user services, input products, geolocation and analysis of data, as well as provenance and Digital Object Identifier (DOI) of the product attached to the root group (the file). The attributes listed in Table 4 are not described further in this user guide.

1.2   LEO-LST Product

The LEO-LST data product consists of Land Surface Temperature (LST) and LST error estimate and is produced on global climate modeling grids at 0.25, 0.5 and 1 degree resolution on monthly time steps since 2002.

1.3   Product Availability

The LEO-LST product will be made available at the NASA Land Processes Distributed Active Archive Center (LPDAAC), https://earthdata.nasa.gov/ and can be accessed via the Earthdata search engine.

2 LEO-LST Product

2.1   Algorithm Description
2.1.1   Regridding

The process for resampling the original 0.05° resolution LST grids to coarser climate modeling grids of 0.25°, 0.5°, and 1° resolution does simply involve averaging the 0.05° grid cells to the coarser resolution. This would only be valid if the scene was homogeneous in emissivity with low LST variation, the LST and emissivity were uncorrelated, and their distribution was symmetrical about the mean value. Instead we recaulcate the effective surface radiance as a sum of individual scene elements, n, within each 0.25°, 0.5°, and 1° grid cell as follows:

$$\bar{R}_\lambda = \bar{\varepsilon}_\lambda \cdot \bar{B}_\nu(\bar{T}_s) = \frac{1}{n}\sum_{i=1}^{n} \varepsilon_{i,\lambda} \cdot B_\lambda(T_{i,s}) \qquad 1$$

Where ε_λ is emissivity for wavelength, λ; T_s is surface temperature (LST); and B_λ is the Planck function:

$$B_\lambda = \frac{c_1}{\pi\lambda^5}\left(\frac{1}{\exp\left(\frac{c_2}{\lambda T}\right) - 1}\right) \qquad 2$$

$c_1 = 2\pi hc^2 = 3.74 \cdot 10^{-16}$ W·m² (1st radiation constant)

h $= 6.63 \cdot 10^{-34}$ W·s^2 (Planck's constant)

c2 $= $ h·c/k $= 1.44 \times 10^4$ µm·K (2nd radiation constant)

k $= 1.38 \times 10^{-23}$ W·s·K^{-1} (Boltzmann's constant)

c $= 2.99 \cdot 10^8$ m·s^{-1} (speed of light)

The final LST for the respective grid cell, *i*, is then computed by inverting the Planck function and accounting for the surface emissivity for that pixel:

$$LST_i = B_\lambda^{-1}/\bar{\varepsilon}_\lambda \qquad\qquad 3$$

The processing steps involved in producing the LEO-LST product are outlined schematically in Figure 2, and a list of the inputs are listed in Table 1.
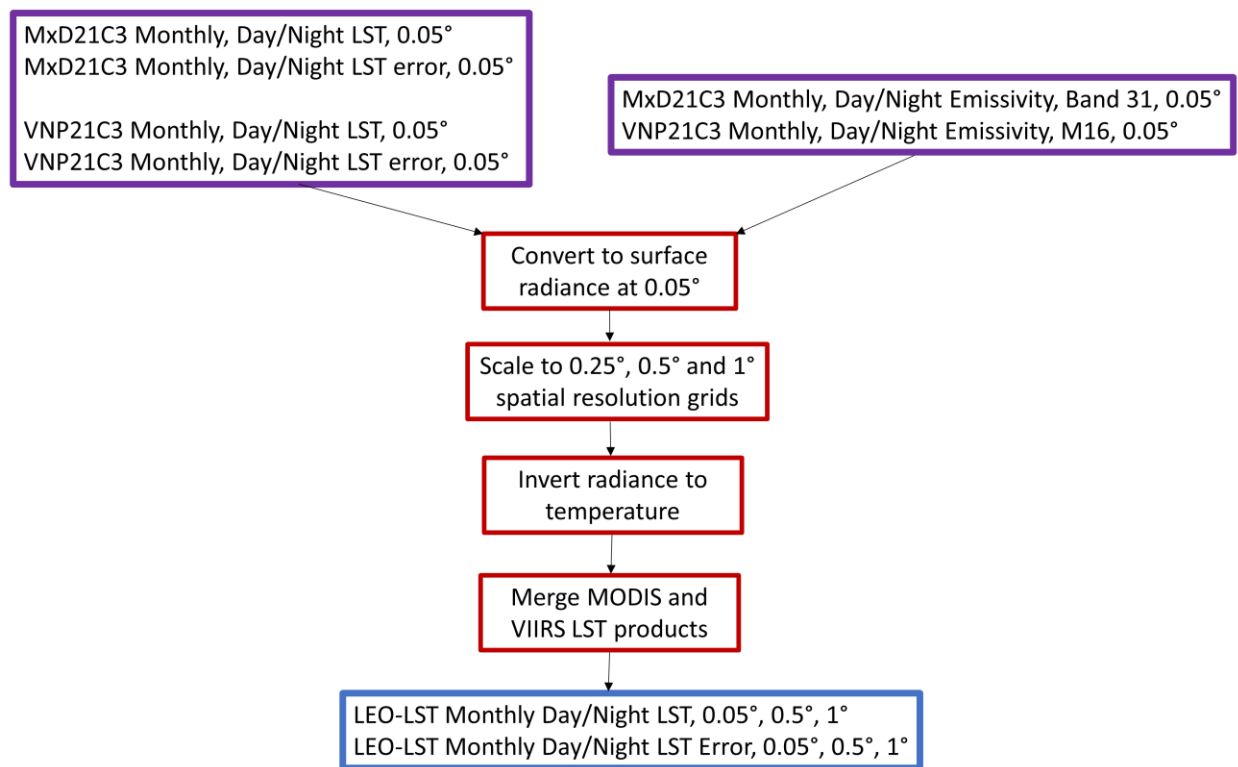

Figure 2. Conceptual diagram describing computation of LEO-LST.

Table 1: Input datasets required to produce the LEO-LST product.

Input Data Set	Long Name	Data Used
MYD21C3 C6.1	MODIS MYD21 Monthly Climate Modeling Grid (CMG) Collection 6.1	Daytime LST Daytime LST error Nighttime LST Nighttime LST error
VNP21C3 C2	VIIRS VNP21 Monthly Climate Modeling Grid (CMG) Collection 2	Daytime LST Daytime LST error Nighttime LST Nighttime LST error
CAMELv2	Combined ASTER and MODIS Emissivity for Land version 2.0	Emissivity

2.1.2 *Combining the VIIRS and MODIS LST products*

During overlap periods of MODIS and VIIRS data (2011-2023) we combine the two products using a "combination of states of information" approach (Tarantola 2005). The question of how to combine different sources of information is a question common to many areas of science. In general, if we have N unbiased estimates of a quantity d, we combine these estimates by taking a weighted average. A systematic approach to developing the weighting rule and error estimation is through "combination of states of information". If $d1$ and $d2$ are two estimates of the same state with uncertainties $\delta 1$ and $\delta 2$, then the weights are simply proportional to the inverse of these variances, and normalized to add up to one. The variances combine to provide an error of the combined estimate. These rules extend with matrix logic to allow for all the correlations of the data in space and time that may need to be accounted for. For example, once the LST uncertainty is known for each pixel on a scene using for the MODIS and VIIRS products, we can write the weighted mean LST as:

$$\overline{LST} = \frac{1}{(w1 + w2)} (w1 \cdot LST_{MYD21} + w2 \cdot LST_{VNP21}) \qquad (2)$$

where $w1$ and $w2$ are weighting factors based on the LST uncertainty for each product, δ, as follows: $w = 1/\delta^2$, and the combined uncertainty of the weighted mean LST product is $\delta LST = (1/(w1 + w2))^{1/2}$.

2.2 Scientific Data Sets (SDS)

The LEO-LST product contains 14 scientific data sets (SDSs): Day and Nighttime LST and associated errors for each grid resolution (ODG = One Degree, HDG = Half Degree, QDG =

Quarter Degree). Details of each SDS including data type and units are shown in Table 2, and the associated attributes of each SDS is shown in Table 3.

Table 2. The Scientific Data Sets (SDS) in the LEO-LST product.

Field Name	Resolution	Type	Unit	Scale factor
LST_Day_ODG	1.0°	int16	Kelvin	0.02
LST_Day_err_ODG	1.0°	int8	Kelvin	0.04
LST_Night_ODG	1.0°	int16	Kelvin	0.02
LST_Night_err_ODG	1.0°	int8	Kelvin	0.04
LST_Day_HDG	0.5°	int16	Kelvin	0.02
LST_Day_err_HDG	0.5°	int8	Kelvin	0.04
LST_Night_HDG	0.5°	int16	Kelvin	0.02
LST_Night_err_HDG	0.5°	int8	Kelvin	0.04
LST_Day_QDG	0.25°	int16	Kelvin	0.02
LST_Day_err_QDG	0.25°	int8	Kelvin	0.04
LST_Night_QDG	0.25°	int16	Kelvin	0.02
LST_Night_err_QDG	0.25°	int8	Kelvin	0.04
Lat	0.25°	Float	Decimal degrees	n/a
Lon	0.25°	Float	Decimal degrees	n/a

Table 3. The attributes assigned to each dataset.

Field Name	Type	Unit	Field Data
long_name	string		
units	string		
Format	String		scaled
coordsys	string		cartesian
Valid_range	Float		
_FillValue	Float		
_Scale	Float		
_Offset	Float		

2.3   Attributes

Archived with the SDS are attributes (metadata) describing characteristics of the data. Contents of these attributes were determined and written during generation of the product at JPL and are used in archiving and populating the database at the LPDAAC to support user services. They are stored as very long character strings in parameter value language (PVL) format. Descriptions of the attributes are given here to assist the user in understanding them. The product specific metadata in Table 4 give details on ancillary data sets.

Table 4. Standard attributes included in all LEO-LST products.

Name	Type	Size	Example
AlgorithmVersion	String	variable	001
DataResolution	String	variable	Climate Modeling Grids: one, half, quarter degrees
DayNightFlag	String	variable	n/a
EastBoundingCoordinate	LongFloat	8	
IdentifierProductDOI	String	variable	10.5067/MEaSUREs/LSTE/LEOLSTCMG30.001
IdentifierProductDOIAuthority	String	variable	https:/doi.org
LocalGranuleID	String	variable	
LongName	String	variable	Low Earth Orbit Land Surface Temperature Monthly Global Gridded V001
NorthBoundingCoordinate	LongFloat	8	
PlatformShortName	String	variable	Aqua, SNPP
ProductionTime	String	variable	
Project	String	variable	MEaSUREs
RangeBeginningDate	String	variable	
RangeBeginningTime	String	variable	
SatelliteInstrument	String	variable	Imager
ShortName	String	variable	LEOLSTCMG30
VersionID	String	variable	
SouthBoundingCoordinate	LongFloat	8	
WestBoundingCoordinate	LongFloat	8	

2.4 LST uncertainty

A key requirement of the LEO-LST is accurate knowledge of uncertainties from the various contributing products. Uncertainties must be rigorously estimated for a variety of different conditions on a pixel-by-pixel basis before they can be merged and incorporated into a time series of measurements of sufficient length, consistency, and continuity to adequately meet the science requirements of an Earth System Data Record(ESDR). Observing System Simulation Experiments (OSSEs) provide a rigorous approach to prepare for assimilation of data from new observing systems and to accelerate their application to operational prediction (Hoffman and Atlas 2016). An OSSE for TIR data termed the Temperature Emissivity Uncertainty Simulator (TEUSim) has been developed to quantify uncertainties in LST&E retrievals from a variety of algorithms and observing system characteristics (Hulley et al. 2012), with a schematic shown in Figure 3.
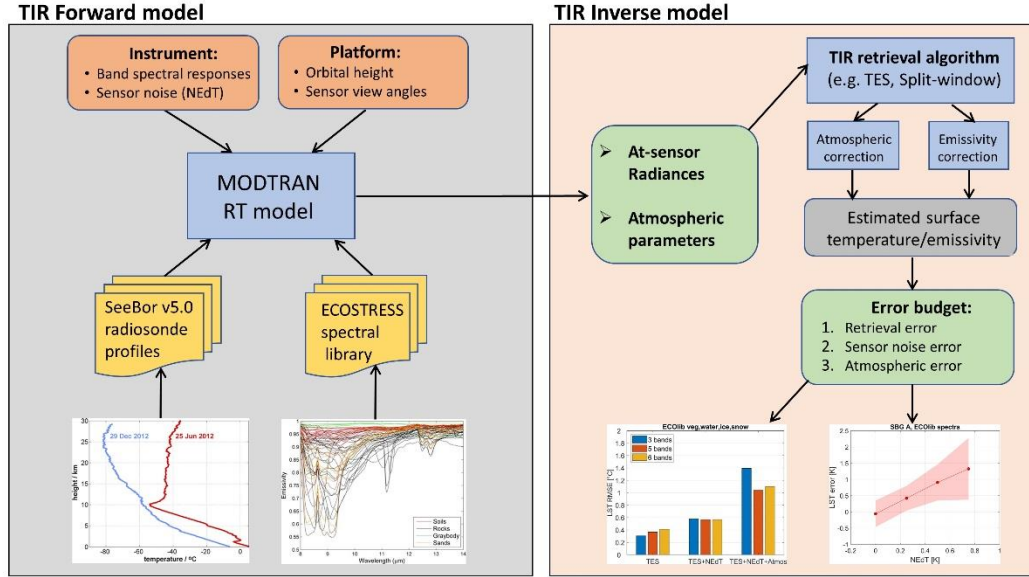
Figure 3. Schematic of the TIR OSSE used to model LST uncertainties in the LEO-LST product. The OSSE uses MODTRAN simulations with a global radiosonde database and ECOSTRESS spectral library to represent a wide range of different conditions. Here the error budget includes contributions from the retrieval algorithm (TES), sensor noise (NEdT) and atmospheric correction error (assuming 10% RH and 2 K Tair random error) for a sensor modeled with 3, 5, and 6 TIR bands in the 8-12 µm range.

These include random errors (instrument noise), systematic errors (calibration), and spatio-temporally correlated errors (atmosphere). The sections below provide details of the TIR OSSE and application for use with the MEaSUREs LST products.

The TEUSim is initialized with a sensor's specific instrument and observing characteristics including instrument noise per band (NEdT), orbital height, viewing geometry, number of TIR bands, and type of LST&E algorithm. The MODTRAN 6.0 radiative transfer model is used for the simulations with a global set of radiosonde profiles (SeeBor V5.0) and surface emissivity spectra (ECOlib) (Meerdink et al. 2019) representing a broad range of atmospheric conditions and a wide variety of surface types. This approach allows the retrieval algorithm to be easily evaluated under realistic but challenging combinations of surface/atmospheric conditions. The outputs include a full error budget of LST error sources computed from the modeled inputs and the retrieved surface parameters including errors from 1) algorithm, 2) NEdT, 3) atmospheric correction, and 4) calibration error.

The total uncertainties generated from TEUSim were parameterized according to satellite view angle (SVA), total water vapor column (TCW), and surface type using a least squares method fit to a quadratic function as follows:

$$\delta LST_{GOES} = a_o + a_1 TCW + a_2 SVA + a_3 TCW \cdot SVA + a_4 TCW^2 + a_5 SVA^2 \qquad (1)$$

Where δLST is the LST uncertainty (K) and a_i are the land cover dependent regression coefficients. Using this parameterization LST uncertainties can be estimated on a pixel-by-pixel basis for any given sensor.

Figure 4 shows an example of the LST uncertainty estimated from TEUSim for the LEO-LST product at 0.25 degree resolution. LST uncertainties typically increase with increasing atmospheric water vapor content which is clearly seen in this image over the tropics and sub-tropical regions. The same methodology has been applied to the GEO LST product.
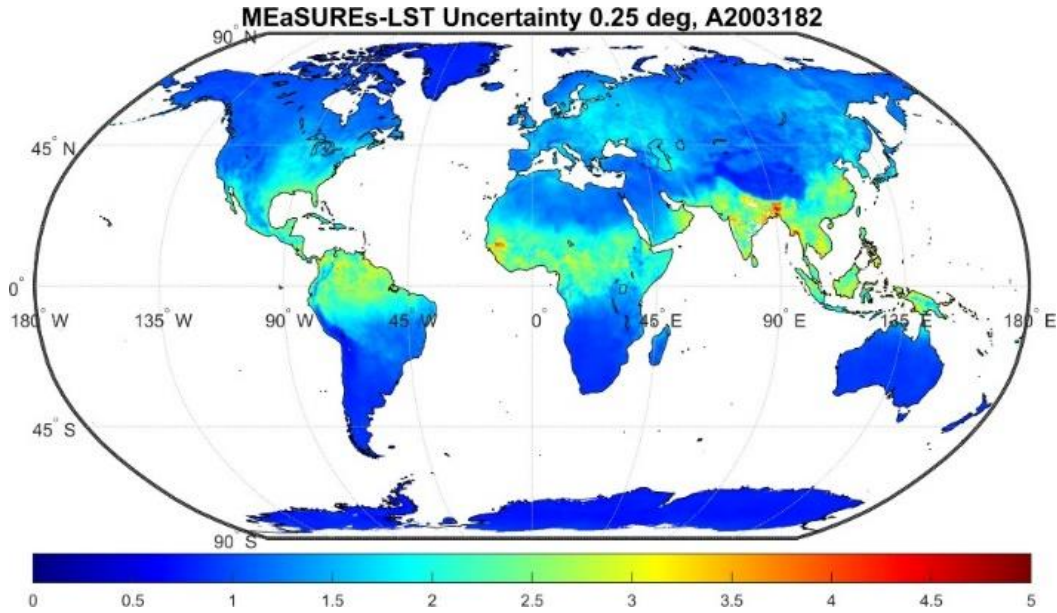

Figure 4. Example LST uncertainty included within the LEO-LST product at 0.25 degree resolution. LST uncertainties typically increase with increasing atmospheric water vapor content which is clearly seen in this image over the tropics and sub-tropical regions.

3   References

Hulley, G., Malakar, N., Islam, T., & Freepartner, R. (2017). NASA's MODIS and VIIRS Land Surface Temperature and Emissivity Products: A Consistent and High Quality Earth System Data Record. *Ieee Geoscience and Remote Sensing Letters, 11*, 522-535

Islam, T., Hulley, G.C., Malakar, N.K., Radocinski, R.G., Guillevic, P.C., & Hook, S.J. (2017). A Physics-Based Algorithm for the Simultaneous Retrieval of Land Surface Temperature and Emissivity From VIIRS Thermal Infrared Data. *Ieee Transactions on Geoscience and Remote Sensing, 55*, 563-576

Malakar, N., & Hulley, G.C. (2016). A water vapor scaling model for improved land surface temperature and emissivity separation of MODIS thermal infrared data. *Remote Sensing of Environment, 182*, 252-264

Tarantola, A. (Ed.) (2005). *Inverse Problem Theory and Methods for Model Parameter Estimation*: Society of Industrial and Applied Mathematics (SIAM), and Springer-Verlag

Anderson, M.C., Hain, C.R., Wardlow, B., Mecikalski, J.R., & Kustas, W.P. (2011a). Evaluation of a drought index based on thermal remote sensing of evapotranspiration over the continental U.S. *Journal of Climate, 24*, 2025-2044

Anderson, M.C., Kustas, W.P., Norman, J.M., Hain, C.R., Mecikalski, J.R., Schultz, L., Gonzalez-Dugo, M.P., Cammalleri, C., d'Urso, G., Pimstein, A., & Gao, F. (2011b). Mapping daily evapotranspiration at field to continental scales using geostationary and polar orbiting satellite imagery. *Hydrology and Earth System Sciences, 15*, 223-239

Dousset, B., & Gourmelon, F. (2003). Satellite multi-sensor data analysis of urban surface temperatures and landcover. *Isprs Journal of Photogrammetry and Remote Sensing*, 58, 43-54

Dousset, B., Gourmelon, F., Laaidi, K., Zeghnoun, A., Giraudet, E., Bretin, P., Mauri, E., & Vandentorren, S. (2011). Satellite monitoring of summer heat waves in the Paris metropolitan area. *International Journal of Climatology*, 31, 313-323

French, A.N., Schmugge, T.J., Ritchie, J.C., Hsu, A., Jacob, F., & Ogawa, K. (2008). Detecting land cover change at the Jornada Experimental Range, New Mexico with ASTER emissivities. *Remote Sensing of Environment, 112*, 1730-1748

Hain, C.R., Crow, W.T., Mecikalski, J.R., Anderson, M.C., & Holmes, T. (2011). An intercomparison of available soil moisture estimates from thermal infrared and passive microwave remote sensing and land surface modeling. *Journal of Geophysical Research-Atmospheres*, 116

Hall, D.K., Comiso, J.C., DiGirolamo, N.E., Shuman, C.A., Key, J.R., & Koenig, L.S. (2012). A Satellite-Derived Climate-Quality Data Record of the Clear-Sky Surface Temperature of the Greenland Ice Sheet. *Journal of Climate*, 25, 4785-4798

Hook, S.J., Dmochowski, J.E., Howard, K.A., Rowan, L.C., Karlstrom, K.E., & Stock, J.M. (2005). Mapping variations in weight percent silica measured from multispectral thermal infrared imagery - Examples from the Hiller Mountains, Nevada, USA and Tres Virgenes-La Reforma, Baja California Sur, Mexico. *Remote Sensing of Environment, 95*, 273-289

Hulley, G., Veraverbeke, S., & Hook, S. (2014). Thermal-based techniques for land cover change detection using a new dynamic MODIS multispectral emissivity product (MOD21). *Remote Sensing of Environment*, 140, 755-765

Luvall, J., Quattrochi, D.A., Rickman, D., & Estes, M.G. (Eds.) (2015). Urban Heat Islands: Encyclopedia of Atmospheric Sciences

NASA (2005). Exploring our Planet for the Benefit of Society, NASA Earth Science and Applications from Space, Strategic Roadmap, http://images.spaceref.com/news/2005/earth_roadmap.pdf

NASA (2011). NASA Earth Science Data Records Programs, http://science.nasa.gov/earth-science/earth-science-data/Earth-Science-Data-Records-Programs/#ESDR_uncertainty_analysis

Rhee, J., Im, J., & Carbone, G.J. (2010). Monitoring agricultural drought for arid and humid regions using multi-sensor remote sensing data. *Remote Sensing of Environment, 114*, 2875-2887

Schneider, P., & Hook, S.J. (2010). Space observations of inland water bodies show rapid surface warming since 1985. *Geophysical Research Letters*, 37

Seemann, S.W., Borbas, E.E., Knuteson, R.O., Stephenson, G.R., & Huang, H.L. (2008). Development of a global infrared land surface emissivity database for application to clear sky sounding retrievals from multispectral satellite radiance measurements. *Journal of Applied Meteorology and Climatology, 47*, 108-123

Semmens, K.A., Anderson, M.C., Kustas, W.P., Gao, F., Alfieri, J.G., McKee, L., Prueger, J.H., Hain, C.R., Cammalleri, C., Yang, Y., Xia, T., Sanchez, L., Alsina, M.M., & Velez, M. (2016). Monitoring daily evapotranspiration over two California vineyards using Landsat 8 in a multi-sensor data fusion approach. *Remote Sensing of Environment*, 185, 155-170

Susskind, J., & Blaisdell, J. (2008). Improved surface parameter retrievals using AIRS/AMSU data. Proc. SPIE, 6966, DOI: 10.1117/1112.774759

Vaughan, R.G., Hook, S.J., Calvin, W.M., & Taranik, J.V. (2005). Surface mineral mapping at Steamboat Springs, Nevada, USA, with multi-wavelength thermal infrared images. *Remote Sensing of Environment, 99*, 140-158

Yao, Z.G., Li, J., Li, J.L., & Zhang, H. (2011). Surface Emissivity Impact on Temperature and Moisture Soundings from Hyperspectral Infrared Radiance Measurements. *Journal of Applied Meteorology and Climatology, 50*, 1225-1235